

DESIGN CONSIDERATIONS FOR THE 4GLS XUV-FEL

B. W. J. McNeil*, G. R. M. Robb, University of Strathclyde, Glasgow G4 0NG, UK
 N. R. Thompson, J. Jones and M. W. Poole,

ASTeC, Daresbury Laboratory, Warrington WA4 4AD, UK

C. K. M. Gerth, Deutsches Elektronen-Synchrotron DESY, D-22603 Hamburg, Germany

Abstract

An XUV Free-Electron Laser operating in the photon energy range 10-100eV is a key component of the proposed 4th Generation Light Source (4GLS) at Daresbury Laboratory in the UK. The current design proposal is an amplifier FEL seeded by a High Harmonic Generation (HHG) source. In this paper we present and discuss the considerations that led to the current design. We also present 3D simulation results that illustrate the potential radiation output characteristics.

INTRODUCTION

The Fourth Generation Light Source (4GLS) proposed for the UK's Daresbury Laboratory is designed to be a user facility to complement existing facilities within both the UK and Europe [1]. The 4GLS sources will provide synchronised ultra-high brightness pulsed radiation covering the FIR to the XUV regions of the spectrum. Previous FEL design considerations and the present design are discussed in this paper. The present design for the XUV uses an HHG seeded, high-gain FEL amplifier that will cover the photon energy range 10-100eV. Design work for a VUV source is considered elsewhere [2].

DESIGN HISTORY

The XUV FEL branch of the 4GLS proposal began as a rather flexible specification for a coherent FEL source operating in the photon energy range 10-100 eV. Initially, attempts were made to design an FEL operating with a monoenergetic electron beam of 600 MeV corresponding to the main Energy Recovery branch and with a single undulator beam-line [3]. For a normal undulator of fixed period, tuning could therefore only be carried out by changing the undulator gap. At this beam energy it was not possible to achieve sufficiently short saturation lengths toward the higher photon energies while maintaining sensible undulator gaps at the lower photon energies.

A twin undulator, HHG seeded FEL scheme that had two separate modes of operation was also investigated. The two undulators were placed colinearly, with the first having a longer period than the second. In the first mode of operation, which would cover the lower photon energies, the first undulator acts as a high gain FEL amplifier seeded by an HHG source and achieves saturation in a relatively short length. This is possible as HHG sources currently

attain peak powers only approximately one to two orders of magnitude below FEL saturation powers for the photon energies 10eV and 50 eV respectively. The second mode of operation would use the second wiggler tuned to an harmonic of the first in an HGHG type configuration, to cover the higher photon energies. Design of such a scheme is quite complex and is complicated in the case of the first, lower photon energy mode of operation by the radiation transport out of the first undulator. Due to diffraction, the radiation cannot be transported through the second undulator and must be extracted at the end of the first undulator for transport to the experimental areas. A simpler option is to introduce further electron acceleration and electron energy tuning as described in the next section.

PRESENT DESIGN

The present design concept for 4GLS incorporates three distinct electron beams driving three different FELs and a range of spontaneous sources. The first branch is a 50 MeV beam for driving an IR FEL oscillator operating at $3 - 75 \mu\text{m}$. The second and third branches are of higher energies at 600 MeV and 750-950 MeV respectively. The 600 MeV branch is of high average current supplying 80 pC pulses at up to 1.3 GHz and operating in an energy recovery mode. This branch will drive spontaneous sources and an FEL operating in the VUV [2]. The third 750-950 MeV branch is designed to give the high peak currents (1.5 kA, 1 nC pulses at 1-10 kHz) necessary to drive a single pass high gain FEL operating in the XUV. A schematic of the current conceptual design for the 4GLS XUV FEL is shown in Fig. (1). Only those components that have direct relevance to the XUV FEL are shown. From the photo-cathode gun, electron pulse acceleration is achieved in three separate stages by superconducting linac modules. Electron pulse compression is carried out in two stages between the main accelerator modules and is enhanced by a 3rd harmonic system. Not shown is the high average current energy recovery branch that has a separate 10 MeV photo-injector and shares the common 590 MeV accelerator stage. The different injector energies for the two branches mean that at the end of the 590 MeV linac the high average current branch has an energy of 600 MeV, while the high peak current branch has energy 750 MeV. This energy difference allows the two branches to be passively separated by a beam spreader immediately after the 590 MeV accelerator section. While the 600 MeV beam will continue through the spontaneous and VUV FEL sources and then on to energy recovery in the 590 MeV accelerator sec-

* b.w.j.mcneil@strath.ac.uk

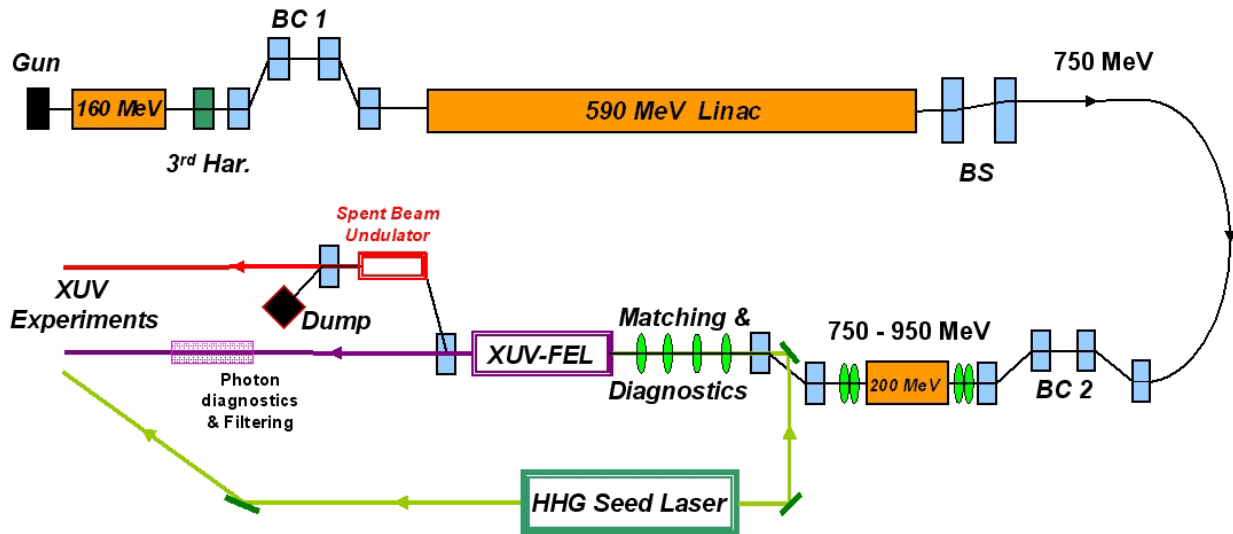


Figure 1: Schematic of the present conceptual design of the XUV FEL branch of 4GLS

tion, the 750 MeV beam takes a different path through a further bunch compressor and a final accelerator stage that may add a further 200 MeV to take the beam energy up to 950 MeV. Following the seeded XUV FEL stage, and before the beam dump, an option to pass the ‘spent’ electrons through a further spontaneous radiation source is included. A high degree of synchronisation is guaranteed between the XUV FEL and this source. The seed laser is shown schematically as a single unit, but may in reality be several High Harmonic Generation lasers. The facility to utilise these lasers as sources synchronised with the XUV FEL for use in user experiments is also included in the design.

Design parameters

The electron beam parameters used for the conceptual design are summarised in Table 1. The additional 200 MeV

Table 1: XUV FEL parameters.

Pulse energy	750-950 MeV
Peak current	1.5 kA
Pulse charge	1 nC
Normalised emittance	2π mm-mrad
Relative RMS energy spread	0.1%

accelerator module outside of the main ERL branch has significant beneficial effects. The additional beam energy tuning it affords, in addition to undulator gap tuning, allows one fixed period undulator to generate sufficient FEL coupling to achieve saturation over the design photon energy range 10-100 eV. Such tuning would be difficult to achieve by energy variation in the upstream injector, ERL accelerator and beam spreader sections which benefit from fixed energy operation. The parameters of Table 1 are used to optimise the undulator and focussing lattice that will cover the design photon energy range 10-100 eV. A Pure Perma-

nent Magnet (PPM) undulator has been chosen at this conceptual design stage although peak on-axis undulator fields may be improved by using a hybrid system. Hybrid undulators will be considered further as a future design option, as will variable polarisation undulators for the final few gain lengths such as the APPLE-II and APPLE-III type undulators. The magnetic field on axis of a PPM type undulator of period λ_w and pole gap g is given by [4]:

$$B_w = 2B_r \frac{\sin(\pi/M)}{(\pi/M)} (1 - \exp(-2\pi h/\lambda_w)) \times \exp(-\pi g/\lambda_w), \quad (1)$$

where the remnant field $B_r = 1.3$, the number of blocks per period $M = 4$ and the block height as a fraction of undulator period $h = 1/2$. A minimum gap is set at $g = 10$ mm.

The FEL design formulae of Xie [5] were used for the first parameter optimisation for generation of 100 eV photons. Table 2 gives the results of the optimisation. This optimisation is limited by, and fulfills, the requirement that the FEL must also be able to lase generating 10 eV photons at minimum undulator gap of 10 mm with electron beam energy of 750 MeV.

Table 2: Optimised parameters of XUV FEL for 100 eV photons using Xie formulae [5].

Undulator period, λ_w	45 mm
Undulator gap, g	~ 28 mm
Beta-function, β	~ 2.2 m
Gain length, l_g	~ 1.44 m
SASE saturation length, L_{sat}	~ 27 m
Seeded saturation length L_{sat}	~ 17 m
Saturation power, P_{sat}	~ 2 GW

Estimation of the seeded saturation length of Table 1 is calculated in the same way as that of the SASE case by

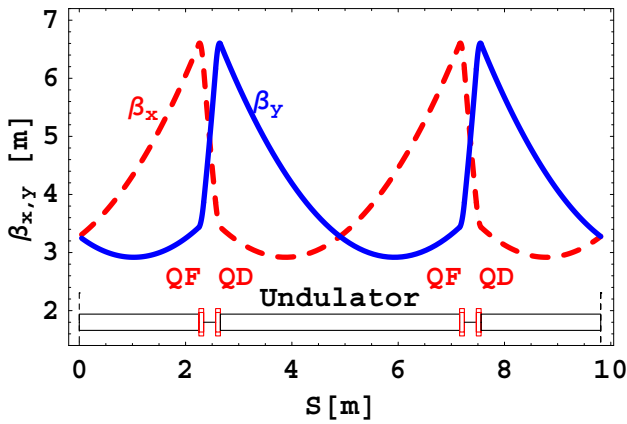


Figure 2: A section of the doublet focussing lattice showing the β -functions (β_x, β_y) in the transverse plane and superimposed schematic of the undulator and quad. positions.

using equation (2) of [5] but with the effective input noise power, $P_n \approx 30\text{W}$, replaced by the seed power $P_{seed} \approx 45\text{ kW}$. This seed power is a conservative estimate based upon current High Harmonic Generation sources [6], and is clearly well above the noise level as required for a good seed source. It is worth noting that for an undulator length of 17 m, the Xie formula estimate that saturation can be achieved via SASE for photon energies up to $\sim 35\text{ eV}$.

The optimised β -function of the Xie formulation describes a constant, uniformly distributed focussing channel. The electron beam is therefore of constant radius $r_b = \sqrt{\epsilon_n \beta / \gamma} \approx 49\mu\text{m}$. The Xie formulae also show that the β -function may be increased from its optimised value of 2.2 m to 4 m with only small effects on the important parameters of Table 2. (E.g. the seeded saturation length is increased by only approximately 1 m.) For the same reasons as discussed elsewhere (see e.g. [7] which uses parameters similar to those discussed here), a discrete, non-uniform focussing lattice is more practical and leads to a design with focussing elements placed between separate undulator sections. Each undulator section has 100 undulator periods and so has total length 4.5 m. This length means a simple FODO lattice will result in significant variation in the β -function over the FODO period, and so a doublet quadrupole focussing lattice has been adopted at this stage. Again, as with [7], a triplet quadrupole lattice was investigated but was found in simulations to offer no significant benefit over the doublet. The undulator sections are separated by 9 undulator periods with each focussing quadrupole of length 2 undulator periods and gradient $\approx 38\text{ T/m}$ placed at the beginning and end of each section. This leaves a length of 5 undulator periods between which other diagnostic, trimming coils, BPMs, phase matchers etc., may be placed.

The combined doublet focussing and undulator lattice used here was modelled and the electron beam at 950 MeV matched to it by the accelerator modelling code MAD [8]. The results are shown in Fig. (2). The mean β -function

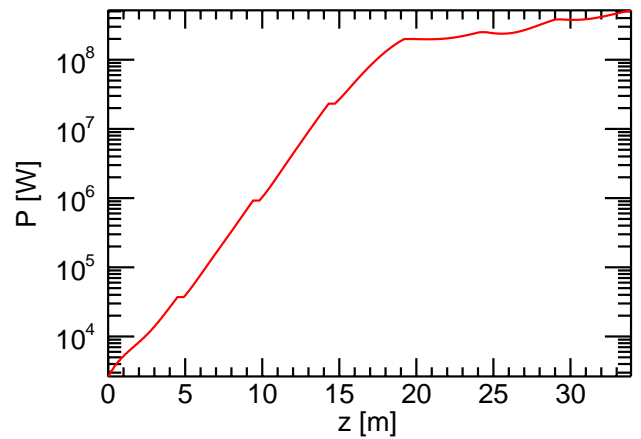


Figure 3: Plot of the average radiation power as a function of distance through the XUV FEL. The average is over the window of width $\sim 500\mu\text{m}$ of Fig. (4).

within the undulators is $\beta = 4\text{ m}$ and throughout the entire lattice, the mean $\beta = 4.8\text{ m}$.

Design simulation

The 3-D FEL simulation code Genesis 1.3 [9] was used in its steady-state mode (neglecting slippage effects) with the above parameters and undulator/focussing lattice. The code estimates a saturation length of $\sim 19.5\text{ m}$ and saturation power of $\sim 2.5\text{ GW}$ which, when the $\sim 1.2\text{ m}$ of gaps between undulator sections is taken into account, is in excellent agreement with the results of the Xie estimates of Table 1.

Genesis 1.3 has also been used to include the effects of pulse propagation. For a total charge of 1 nC and peak current of 1.5 kA, the Gaussian electron pulse has a temporal width of $\sigma_t \approx 266\text{ fs}$. A Gaussian radiation pulse was injected of peak power 60 kW (RMS power $\sim 36\text{ kW}$) coincident with the peak of the current. The radiation pulse had a temporal width $\sigma_t = 30\text{ fs}$, typical of present HHG sources. The radiation was injected to a focus at 2.25 m into the first undulator section. The average FEL power, averaged over a window of width $500\mu\text{m}$, is shown in Fig. (3). It is seen that the power saturates toward the end of the fourth undulator section at $z \approx 19\text{ m}$. This agrees well with the results of the Xie formulation above despite the slightly smaller initial RMS input power. The structure of the radiation pulse power at saturation is plotted in Fig. (4) and shows a well defined pulse structure showing little of the noise associated with SASE. The relative slippage of the radiation with respect to the electron pulse is approximately $4.8\mu\text{m}$ being just over half of the width of the seed $\sigma_z \approx 9\mu\text{m}$ (30 fs). This slippage results in a slight increase in the width of radiation pulse width over that of the seed. Note that only that part of the electron pulse (current of peak 1.5 kA shown superimposed) that has been seeded has had any significant contribution to the FEL lasing. As the interaction proceeds, post saturation of the seeded re-

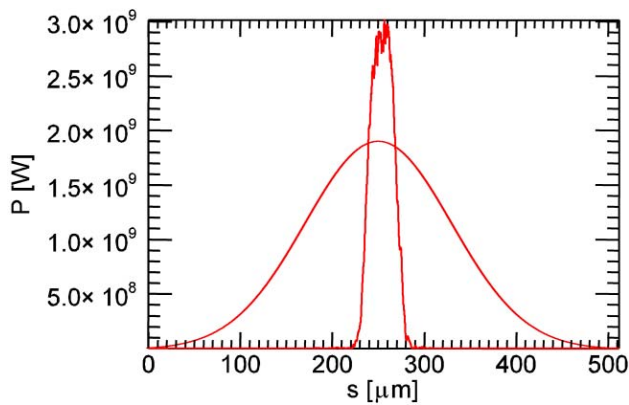


Figure 4: Radiation pulse power at saturation ($z=19$ m) as a function of $s=ct$. The wider electron beam current of peak 1.5 kA is also shown.

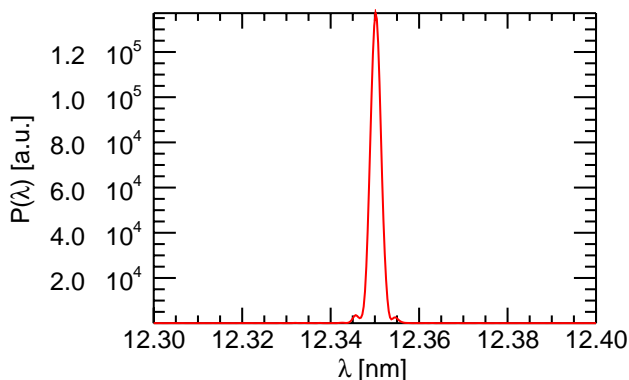


Figure 5: The spectral power at saturation as a function of radiation wavelength λ , confirms the enhanced radiation properties of a seeded FEL over that of SASE.

gion, then the remaining regions of the electron pulse begin to saturate via the SASE mechanism, spreading out from the centre of the electron pulse toward the lower current regions. This accounts, in large part, for the increasing average power for $z \gtrsim 25$ seen in Fig. (3). The improved radiation pulse properties over that of SASE and suggested by the clean radiation pulse structure of Fig. (4) is confirmed in the plot of the spectral power at saturation of Fig. (5). Both the electron pulse current and seed radiation intensity will be subject to relative timing ‘jitter’ and therefore will not always be coincident. If this jitter is the width of the Gaussian electron pulse ($\sigma_t \approx 266$ fs) then the current the seed interacts with is reduced to approximately 910 A. According to the Xie estimates this increases the seeded saturation length from 18 m to 24 m and reduces the saturated power from approximately 2 GW to 1.2 GW. (Of course, the correlation between the interaction current and timing jitter is determined by the shape of the current pulse and will require more detailed simulation of the complete system.)

CONCLUSIONS

The ongoing design work for the 4GLS facility is an iterative process and is initially intended to lead toward a Conceptual Design Report, which will be published in the Spring of 2006, and thence to the Technical Design Report to be published toward the end of 2006. The present design remains a work-in-progress and will undoubtedly evolve further. Crucial to the final design will be a more detailed specification of the proposed HHG seed sources and further analysis of the stability of the FEL operation with respect to timing jitter within the system. Both of these issues will now be more closely studied. The use of other undulator systems that use hybrid magnets and variable polarisation (APPLE) also require further investigation. The former may allow extension of the FEL operation to lower photon energies while the latter will be required to provide users with variable polarised radiation. The current design proposal is relatively simple and therefore will hopefully have an inherent robustness built in that will ensure reproducible and stable operation for users. This also gives the design the scope for future upgrade e.g. addition of accelerator modules to further increase the electron energy or the addition of a modulator undulator for HGHG type operation to higher photon energies. The latter may also provide a fall-back scheme to generate the higher photon energies up to 100 eV in the event that suitable HHG sources for direct seeding are not available.

We acknowledge the support of the CCLRC, and the Scottish Universities Physics Alliance and the valuable contributions of colleagues on the 4GLS International Advisory Committee.

REFERENCES

- [1] M. W. Poole and E. A. Seddon, Proceedings of Particle Accelerator Conference, Knoxville, USA (2005)
- [2] N. R. Thompson and B. W. J. McNeil, *ibid* (2005)
- [3] M. W. Poole and B. W. J. McNeil, Nucl. Inst. Meth. Phys. Res. A, **507**, 489 (2003)
- [4] J. A. Clarke, *The science and technology of undulators and wigglers*, (Oxford University Press, 2004.)
- [5] Ming Xie, Proc. Of 1995 Part. Accel. Conf., 183 (1996)
A MATLAB package for solving and displaying solutions can be found at <http://phys.strath.ac.uk/eurofel/rebs/desXie/desXie.htm>
- [6] Eiji J. Takahash *et al*, IEEE J. OF Selected Topics in Quantum Electron., **10**, 1315 (2004)
- [7] B. Faatz, J. Pflüger, Nucl. Instr. and Meth. A **475**, 603 (2000)
- [8] H. Grote and F. C. Iselin, CERN/SL/90-13(AP) (Rev. 5), <http://hansg.home.cern.ch/hansg/mad/mad8/mad8.html>.
- [9] S. Reiche, Nucl. Inst. and Meth. A **429**, 243 (1999)
- [10] C. Gerth, *et al*, Proceedings of the 26th International Free Electron Laser Conference, Trieste (2004)